Chapter 3

In vitro and *in silico* inhibition studies on Xanthine Oxidase with tea polyphenols

1 Introduction

Molybdenum containing enzymes can be grouped into two classes, namely nitrogenases and hydroxylases (oxo-transferases). This classification is based on the cofactor metal constituents as well as on other cofactors that are required in the electron acceptor domain (Romão, 1998). Nitrogenases catalyze the reduction of molecular nitrogen to ammonia. The electron acceptor domain contains a hetero-metal cofactor (Fe-Mo) and no pterin cofactor. All the molybdenum hydroxylase enzymes possess only Mo as metal ion and a pterin cofactor that consists of a tetrahydropterin core with a dithiolene sidechain and a phosphate group. This pterin is called a molybde-

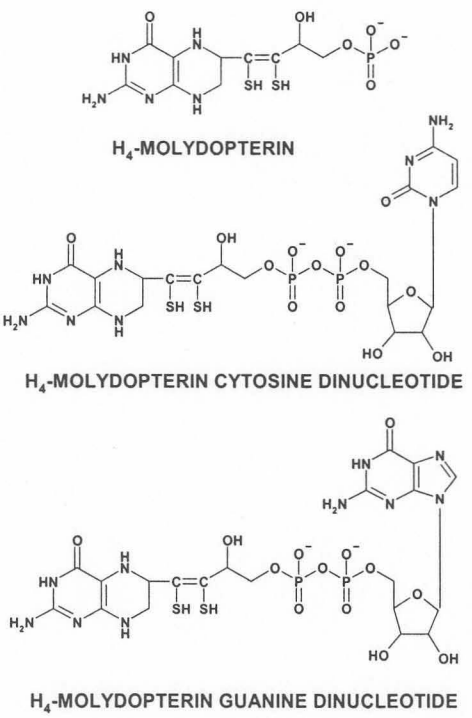

Figure 3.1 Structures of the variant forms of molydopterin. The structures are shown in the tetrahydro state, but they may also occur in the dihydro state *in vivo*.

num cofactor (Moco) and different variations on the cofactor structure do exist. The variant with a guanine linked to the phosphate of the Moco occurs mainly in eukaryotes, while the variant with a cytosine occurs mainly in prokaryotes (Fig. 3.1) (Rajagopalan, 1991). XO isolated from bovine milk has the monophosphate Moco variant.

The molybdenum hydroxylases promotes a variety of two-electron oxidation-reduction reactions whereby the oxygen atom from H_2O is transferred to a substrate at the electron acceptor domain. The remaining reducing equivalents obtained from the H_2O molecule are transferred to an electron acceptor at the electron donating domain (Fig. 3.2). These enzymes are classified into three families on the basis of the reactions they catalyze, as well as the basis of the characteristics of the molybdenum centers. They are (1) the xanthine oxidase family, (2) the sulfite oxidase and nitrate reductase family and (3) the DMSO reductase family. This classification is supported by the amino acid homologies within the protein families (Romão, 1998).

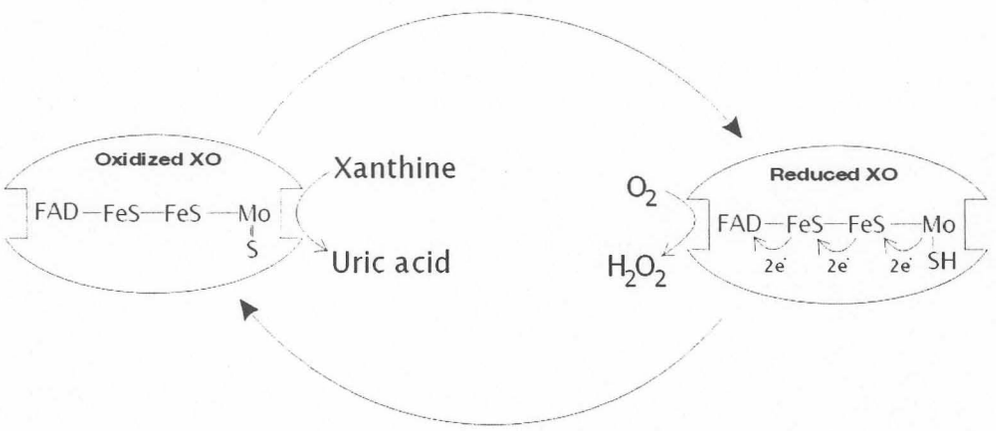

Figure 3.2 A schematic presentation of the ping-pong catalytic action of xanthine oxidase.

The large xanthine oxidase family of enzymes may be considered one of the true hydroxylases. In the electron acceptor domain the Mo is coordinated to an oxygen

(oxo), a sulfur (sulfido) and a water molecule as well as to the substructure dithiolene via the two sulfur atoms. In the complex the $MoOS(H_2O)$ is coordinated in the *fac* orientation. The two sulfurs of the dithiolene forms the equatorial plane of the penta-coordinated square pyramidal complex (Fig. 3.3) and the sulfido forms the apical ligand of the complex. Members of this family have been found broadly distributed within eukaryotes, prokaryotes and archaea. They catalyze the oxidative hydroxy-lation of aldehydes and aromatic hetrocycles in reactions involving C-H bond cleavage.

oxidized enzyme (Mo^{VI}) reduced enzyme (Mo^{IV})

Figure 3.3 The structure of the molybdenum coordination complex. The Mo^{VI} is penta-coordinated in the square pyramidal geometry. The equatorial plane is defined by the two dithiolene sulfurs, oxido and water ligands. The sulfido is in the apical position.

XO is named so because xanthine was thought to be its physiological substrate. Later it was found that XO has a low substrate specificity and it oxidizes many aromatic heterocycles, aldehydes and alcohols. XO has a molecular mass of approximately 300 kDa, and is a homodimer. Besides a molybdenum center and Moco it also possesses two iron-sulfur centers of the 2Fe/2S variety and a flavin adenine dinucleotide (FAD) per subunit (Hille, 1994). Physiologically the enzyme uses NAD^+ as electron acceptor and the enzyme is known as xanthine dehydrogenase (XDH). Under stress conditions it is converted to XO and uses O_2 as electron acceptor. The difference between XDH

and XO is with the electron donator domain and not the xanthine binding electron acceptor domain.

The aldehyde oxido-reductase (AOR) from *Desulfovibro gigas* is the first representative of the xanthine oxidase type enzymes for which the three-dimensional structure is available (Romão, 1995). Although there are differences between XO and AOR, a wealth of information can be extrapolated from AOR about the structure and enzyme reactions of XO. Multiple alignment with the family of XO's from mammalian, insect and fungal sources showed that the AOR amino acid sequence is highly conserved with *ca.* 52% homology and 25% identity, suggesting a close structural relationship (Fig. 3.4) (Romão, 1998). The homology is particularly high in those segments associated with binding of the redox cofactors as well as within residues of the substrate-binding pocket, and for the residues of the substrate tunnel. The segment binding to the cytosine dinucleotide substructure is not conserved because XO, isolated form bovine milk, has the monophosphate variant of the Moco. In Fig. 3.4 it can be seen that the binding segments of the cofactors are well conserved with a high proportion of invariant residues and secondary structures. Interruptions by deletions and insertions occur only in loop regions and at the N- and C-termini. The long deletion of about 400 residues in the AOR structure between residues 176 and 177, corresponds to the FAD (electron donating) domain in the xanthine dehydrogenases and is absent in AOR. This additional domain must be placed, in the XO family of enzymes, somewhere along the extended connecting segment (white part in Fig. 3.5). The FAD binding domain has been tentatively assigned on the basis of mutant studies. A mutation that has received considerable attention, was the Y395F xanthine dehydrogenase from *Drosophila melanogaster*, which has shown to be enzymatically inactive.

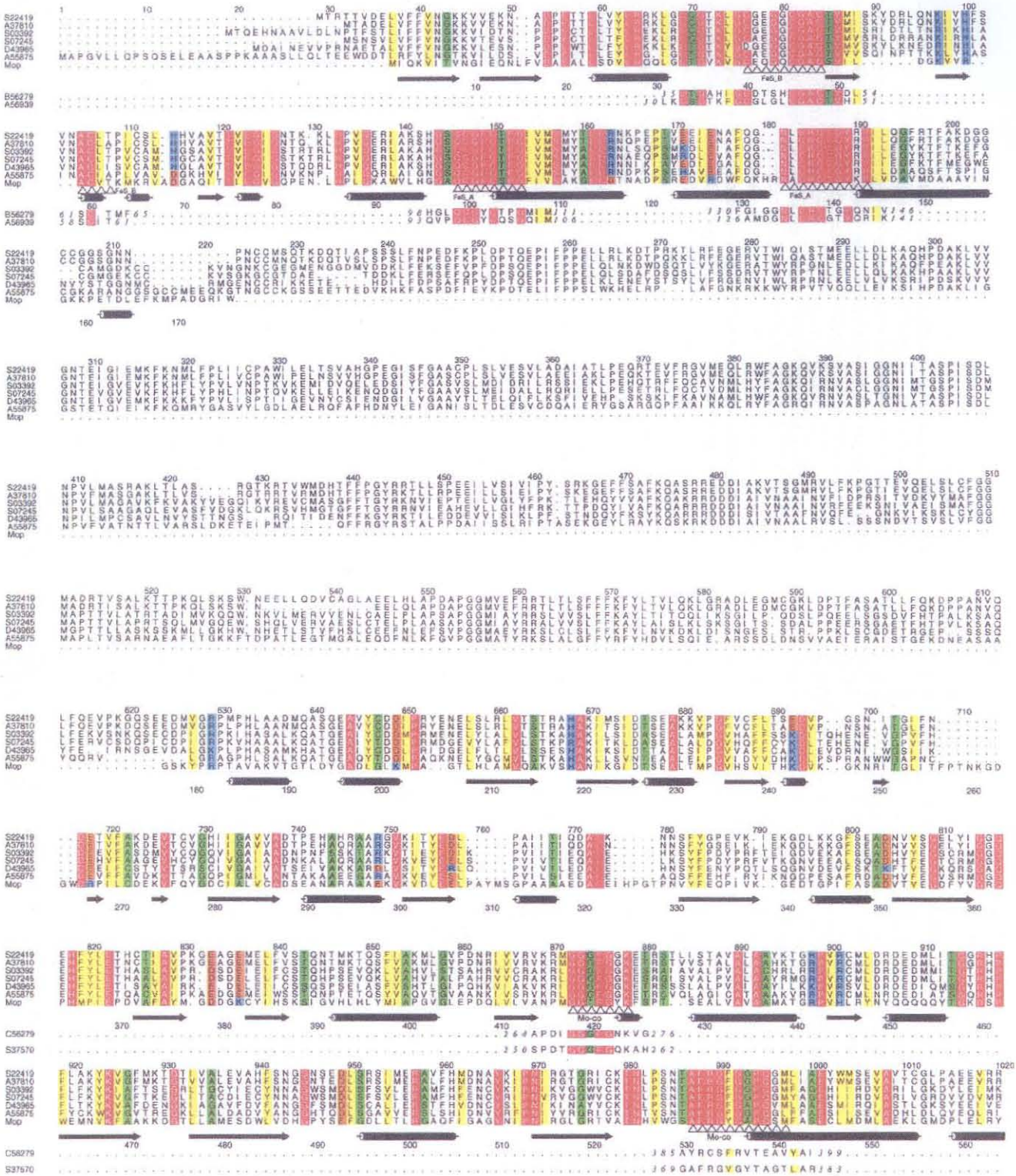
S22419
A37810
S03392
S07245
D43965
A55875
Mop
B56279
A56939
C56279
S37570
C58279
S37570

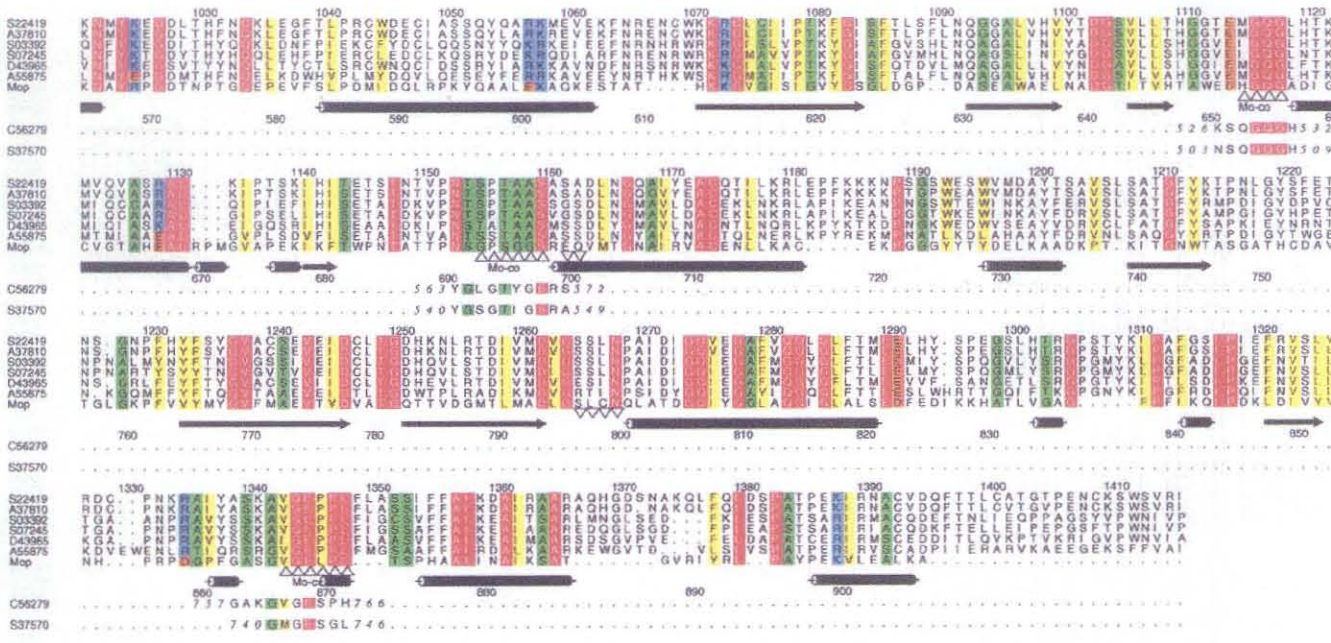

Figure 3.4 Amino acid sequence alignment of Mop (Aldehyde Oxido-reductase) with Xanthine Dehydrogenases. The sequences were taken from the PIR data bank. S22419: mouse xanthine dehydrogenase; A37810: rat xanthine dehydrogenase; SO3392: *Calliphora vicinia* xanthine dehydrogenase; SO7245: *Drosophila melangoster* xanthine dehydrogenase; D43965: *Bombyx mori* xanthine dehydrogenase; A55875: *Ernericillia nidulans* xanthine dehydrogenase. Also included are the partial sequences around the cofactor binding sites of carbon monoxide dehydrogenase from *Pseudomonas carboxydovorans*, B56279, C56279, isoquinoline-1-oxidoreductase from *Pseudomonas diminuta*, A56939 and nicotine dehydrogenase from *Arthrobacter nicotinovorans*, S37570. Alignments were performed with the program PILEUP and ALSCRIPT within The GCG package. Invariant residues are colored red, conserved hydrophobic residues yellow, conserved small neutral residues green, and conserved charged residues brown (negatively charged) and blue (positively charged). The secondary structural elements of β-strands (⟨) and helices (■) and the segments contacting the iron-sulfur clusters and the molydopterin (ΔΔΔΔΔΔΔ), and the cytosine (∇∇∇∇∇∇) are defined as in (Romão, 1995) and marked as shown. (Adapted from (Romão, 1998))

Figure 3.5 Molecular structure of aldehyde oxido-reductase and ligands. The helical and β-sheet secondary structures are drawn as rods and arrows with WebLab ViewerLite. The sulfurs of the cofactors are yellow, and the metal atoms are silver. The substrate binding tunnel is in the middle lower third of the molecule. The view is onto the molybdenum from the approaching substrate. The blue and green domains are the first [2Fe-2S] and second [2Fe-2S] domains respectively. The white domain is the connecting domain where the FAD site of XO and XDH is presumably inserted. The light brown and dark brown domains are the Mo1 and Mo2 domains respectively. The molydopterin cofactor is bound in between the Mo1 and Mo2 domains, seen as a ball and stick model.

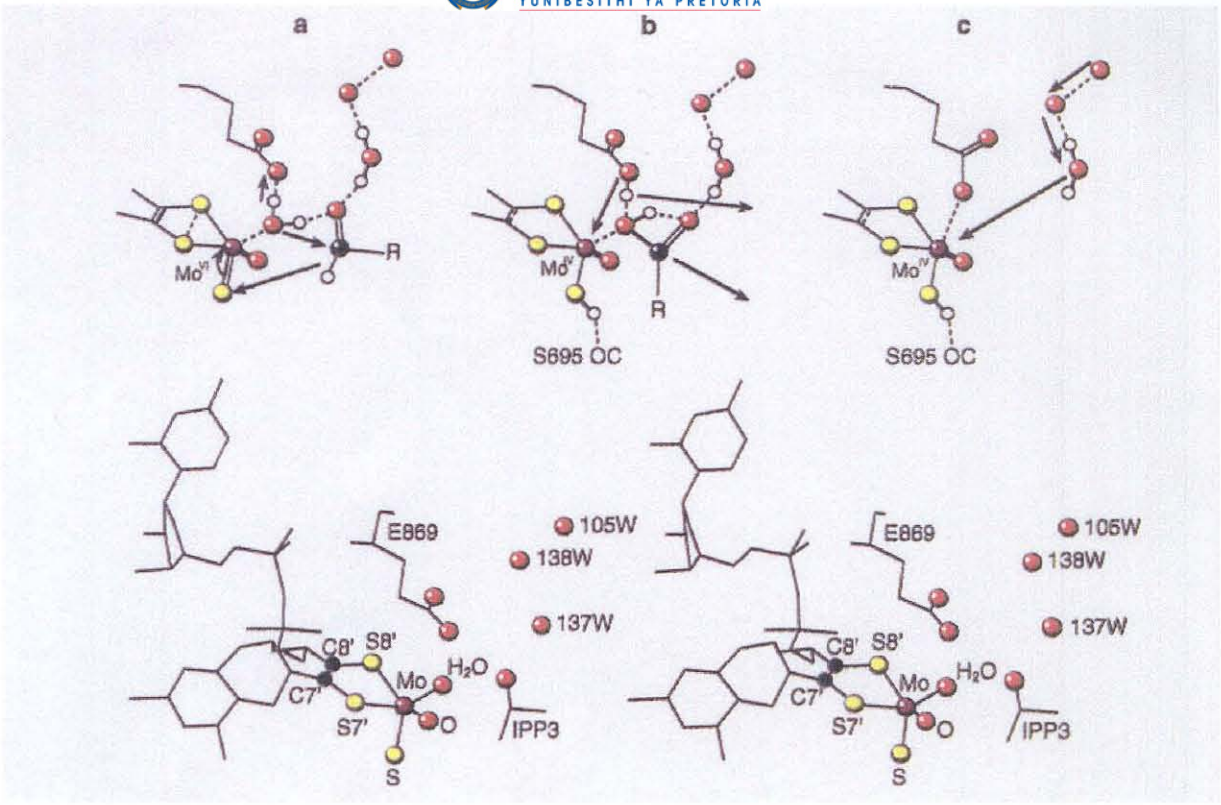

Figure 3.6 The reductive half-cycle of the hydroxylation reaction of AOR and XO.

The close structural relationship and ability of XO to utilize a wide range of aldehydes implies a common mechanism of action for AOR and XO. Furthermore, studies of the structural and spectroscopic properties of the metal cofactors of both enzymes suggest a close similarity. Of particularly significance are the similar electron paramagnetic resonance (EPR) properties of the molybdenum centers of both enzymes. This justifies the interpretation of results obtained from XO on the basis of the structural data for the AOR enzyme.

The reaction of XO follows a typical ping-pong bi-bi mechanism. The ping-pong mechanism for the steady-state formation of uric acid from xanthine can be presented as two independent half-reactions, shown in equations 1 and 2 (Hille, 1994).

reductive half-reaction

$$(XO)_{ox} + Xan + H_2O \rightleftharpoons (XO)_{ox}\bullet Xan \longrightarrow (XO)_{red} + urate \quad (1)$$

oxidative half-reaction

$$(XO)_{red} + O_2 \rightleftharpoons (XO)_{red}\bullet O_2 \longrightarrow (XO)_{ox} + H_2O_2 \text{ (or } O_2^-) \quad (2)$$

Although the mechanism for the reductive half cycle is not entirely certain, the structural data obtained from the three-dimensional structure and spectroscopic data of AOR and XO suggests a mechanism as outlined in Fig. 3.6. The Phe425 of AOR has been exchanged with the homologous Glu in XO (not shown in Fig.3.6). The glutamate is well positioned to bind to the N3, N9 imidium substructures of purines. Water 137 is suggested to be the specific recognition site for N7. The Glu869 serves as proton abstracting base, taking a proton from the water ligand bound to Mo. This provides a metal activated OH- that launches a nucleophillic attack on the C8 of a purine. The C8 of the purine is co-planar with the sulfido group, Mo and the coordinated H_2O such that the educt may be viewed as an open six-membered ring orientated perpendicular to the Mo=O bond. In the next step a hydride from C8 is transferred to the sulfido group, reducing the Mo^{VI} to Mo^{IV} and protonating the sulfido to a sulfhydryl group. The metal bound H_2O is transferred to the C8 upon which Glu869 abstracts the proton leaving a hydroxylated C8. The release of the product from the molybdenum may be facilitated by transient binding of Glu869 to the metal to maintain the penta-coordination. The molybdenum water coordination site may then be refilled from the chain of internal water molecules. At the end of the reductive cycle the Mo^{VI} is reduced to Mo^{IV}.

During the oxidative cycle the reducing equivalents obtained by the Mo-center are transferred to dioxygen at the flavin to form either peroxide or superoxide. These electrons are transferred via the Moco and iron-sulfur centers to the FAD site where it is transferred to molecular oxygen. The reducing equivalents are transferred through the partially conjugated system of the pterin and a hydrogen bond to the first Fe/S center. Electron transfer then proceeds via several covalent bonds and one hydrogen bond towards the second Fe/S center. From here the electrons will flow to FAD as an electron acceptor probably in a similar manner through covalent bonds and conjugated systems. The electron transfers are made possible by redox potential differences and reorganization energies. At the end of the oxidative cycle the Mo^{IV} is oxidized back to Mo^{VI}.

Allopurinol, a structural analogue of xanthine is the best known inhibitor of XO. Allopurinol is converted to oxypurinol in the catalytic center of XO. Both compounds compete with the physiological substrates for the active center of the enzyme. Once oxypurinol has formed a complex with the enzyme, it dissociates very slowly from the active center of the enzyme. Oxypurinol is an efficient tight binding inhibitor of XO and exerts non-competitive type inhibition (Massey, 1970).

The majority of XO inhibitors are heterocyclic aromatic compounds and aldehydes or alcohols that mimic purine and aldehyde substrates of XO. Most of the inhibitors exert non-competitive or mixed type inhibition. Uric acid and 8-bromoxanthine are two compounds that show uncompetitive type inhibition (Hille, 1984), (Radi, 1992). Natural plant products such as polyphenols and coumarins have also been shown to

inhibit XO (Chang, 1995 (c)). Although the types of inhibition for these inhibitors are known, the exact mode of action has not been investigated.

2 Materials and Method

2.1 Materials

XO Grade III from buttermilk (1.2 units/mg), quercetin, kaempferol and allopurinol were purchased from Sigma Chemical Company (St Louis, MO, USA). (+)-C, (-)-EC, (-)-EGC, (-)-ECg and (-)-EGCg were gifts from Mutsui Norin (Tokyo, Japan). All buffer salts and solvents needed for assay or running buffers were of analytical grade.

2.2 Xanthine Oxidase assay

All assays were done aerobically at 20°C. The enzyme activity was measured spectrophotometrically by determining uric acid formation at 295 nm with xanthine as substrate (Kalckar, 1947). The XO assay consisted of 200 µl reaction mixture containing phosphate buffer pH 7.4, 0.05 M; 0.004 U/ml XO and xanthine substrate. The assays that were conducted without inhibitors, were started by addition of the enzyme to the reaction mixture. The reference cuvette was identical and only enzyme was absent. The assay mixture was incubated for 3 minutes and absorbency readings were taken every 20 seconds.

The inhibitor concentrations were selected by assaying at a substrate concentration equal to Km (2.5 µM) (White, 1981). Three inhibitor concentrations were chosen by pre-trails to give approximately 50%, more than 30% and less than 70% inhibition at a substrate concentration equal to Km. All inhibitors were pre-incubated with enzyme for 10 minutes. The reaction was started by addition of the substrate. A substrate

range of 1.25 μM (0.5 Km) to 10 μM (4 Km) was used to avoid substrate inhibition, which was evident above 25 μM xanthine in our assay (Aucamp, 1997). EDTA was added to the assay mixture (33.3 μM for EGC, ECg and EGCg, since color changes were noticed on standing at room temperature or on ice in the dark.

2.3 Molecular modeling of XO inhibitors

Various inhibitors of XO were taken from the literature and modeled in the CORINA software package (http://www2.ccc.uni-erlangen.de/software/corina/free_struct). CORINA generates a low energy conformation structure for each inhibitor or substrate. The 3D structures of the inhibitors were compared in pursuit of identifying a structure-activity relationship and to evaluate the possibilities of designing other XO inhibitors.

3 Results and Discussion

3.1 Inhibition of XO with tea polyphenols

The compounds tested are shown in Table 3.1 together with their K_i, K_I and apparent K_i values and types of inhibition displayed. The Lineweaver-Burk method was used to confirm the K_m of xanthine, the type of inhibition and apparent K_i value of each inhibitor. The K_m value for xanthine was found to be 1.25 μM, (Fig. 3.7). For mixed type inhibition the secondary plots of $1/V_{max}$ vs [I] and slope vs [I] were used to determine K_i and K_I respectively. The secondary plots of the mixed type inhibitor (-)-EC are shown in Fig. 3.8. Linear secondary plots indicate the formation of dead-end complexes and parabolic non-linear plots indicate that more than one inhibitor molecule binds per enzyme. Non-linear secondary plots were only observed for quercetin and kaempferol. The secondary plots of the mixed type inhibitor kaempferol are shown in

Fig. 3.9. The inhibitory constants were estimated from non-linear secondary (plot slope vs [I]). These results will be interpreted after the inhibition model is discussed for better understanding.

Table 3.1 Summary of the kinetic data of the tested polyphenols.

Inhibitor	Type of Inhibition	Apparent K_I (μM)	K_I (μM)	K_i (μM)	K_i/K_I
Allopurinol	Mixed type	0.30	0.24	0.93	3.88
Quercetin	Mixed type	0.25	0.20	0.53	2.65
Kaempferol	Mixed type	0.33	0.17	0.82	4.85
(+)-Catechin	Uncompetitive	303.95	-	303.95	0
(-)-Epicatechin	Mixed type	20.48	24.62	241.02	9.8
(-)-Epigallocatechin	Mixed type	10.66	14.44	25.02	1.73
(-)-Epicatechin gallate	Mixed type	2.86	1.83	28.45	15.55
(-)-Epigallocatechin gallate	Competitive	0.76	0.76	-	∞

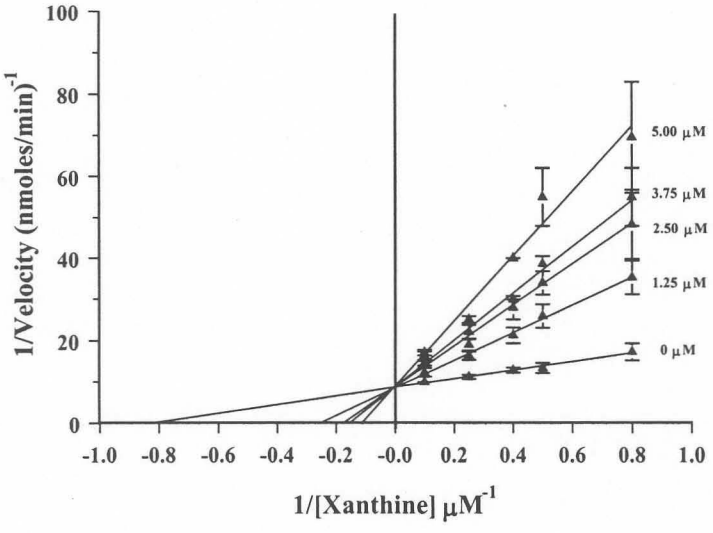

Figure 3.7 The Lineweaver-Burk plot for the inhibition of xanthine oxidase by (-)-EGCg with xanthine as substrate.

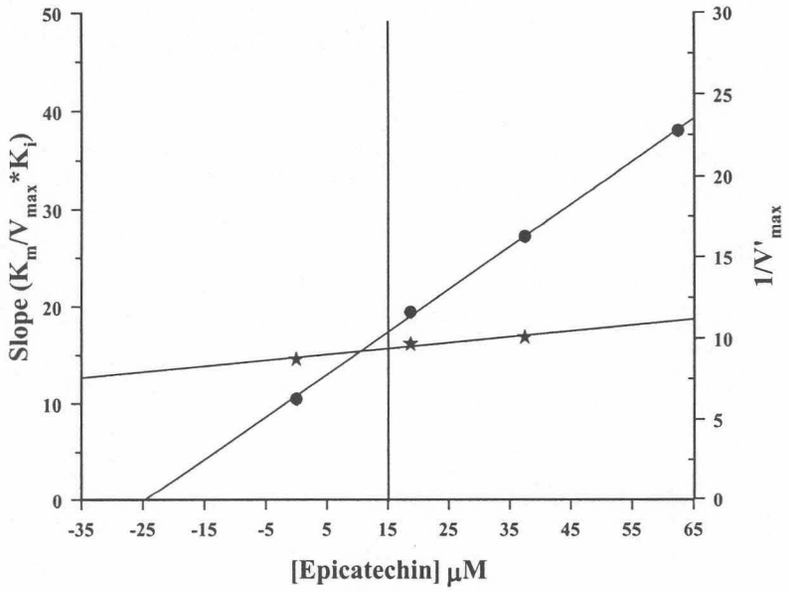

Figure 3.8 The linear secondary plots of the inhibitor (-)-EC. The 1/Vmax vs. [I] plot is represented by the (★) and the Slope vs.[I] plot is represented by (●).

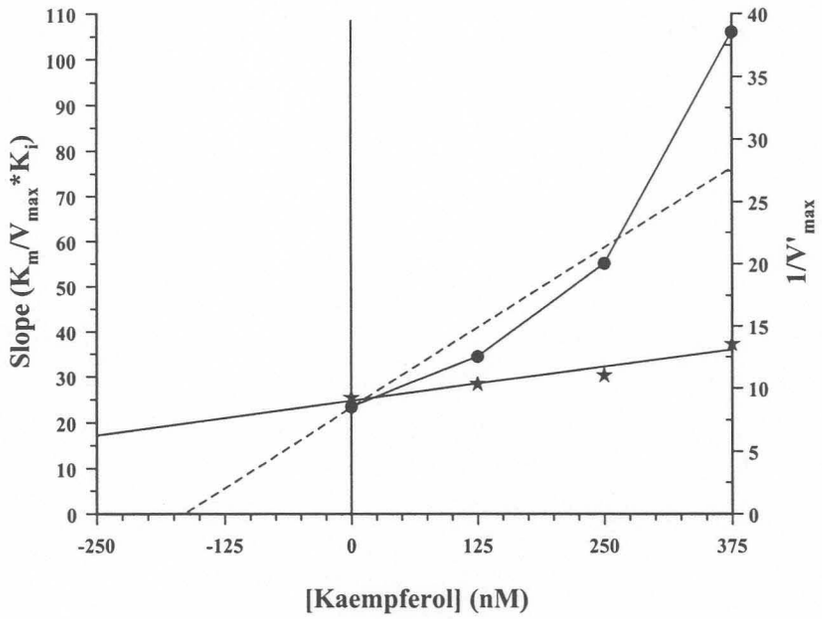

Figure 3.9 The secondary inhibition plots of the inhibitor kaempferol. The 1/Vmax vs. [I] plot is represented by the (★) and the Slope vs.[I] plot is represented by (●).

3.2 Model for structurally similar XO inhibitors

The first requirement for determining a structure-activity relationship is to obtain a model that can explain all the observed activities in a rational manner. Since XO has a ping-pong bi-bi catalytic mechanism, it is unlikely that normal single-substrate equations such as Michaelis-Menten (even under pseudo-single substrate conditions) will give adequate explanation for the inhibition results. This statement can be substantiated with the results obtained with the XO inhibitors, alloxanthine (oxypurinol) and 8-bromoxanthine (Fig. 3.10). The two inhibitors are structurally similar and both have been shown to bind to the electron acceptor domain of XO. Yet alloxanthine shows mixed type inhibition (Massey, 1970) and 8-bromoxanthine uncompetitive inhibition (Hille, 1984). According to single substrate inhibition models, both inhibitors have to bind to the ES complex to exert mixed-type or uncompetitive inhibition. This will

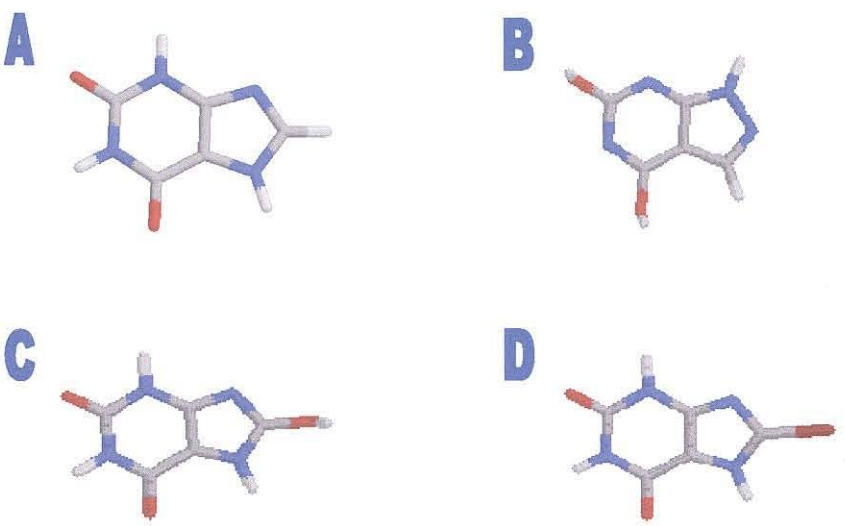

Figure 3.10 The three dimensional structures of the XO substrates, products and their inhibitory analogues. A: Xanthine (substrate), B: alloxanthine / oxypurinol (substrate analogue), C: uric acid (product), D: 8-bromoxanthine (product analogue).

form an ESI enzyme complex, but since both S and I binds to the electron acceptor domain it is impossible to form an ESI complex. Thus single-substrate Michaelis-Menten kinetics is not a suitable model for explaining this inhibition.

In explaining this inhibition behavior, the inhibitors should be seen as competing with the substrate for the electron acceptor domain of the enzyme. The inhibitors simulate "alternative substrates" for the enzyme. This allows the implementation of the mathematical procedures used for explaining the effects of alternative substrates on the enzyme activity for physiological substrates (Huang, 1979). From the schematic presentation of the XO ping-pong bi-bi reaction, it can be seen that there is an oxidized (E_{ox}) and a reduced (E_{red}) form of the enzyme to which competitive inhibitors can bind (Fig. 3.11).

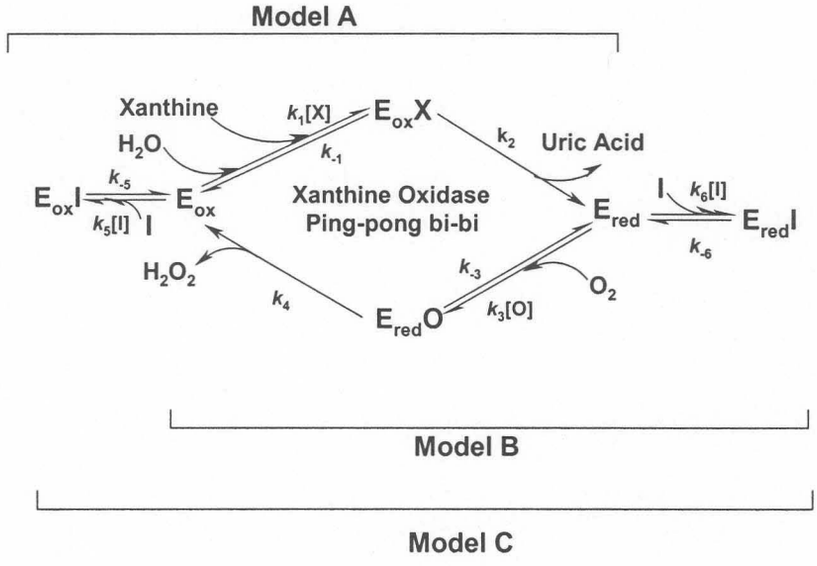

Figure 3.11 A possible model by which the tea polyphenols as well as XO substrate and product analogues exert their inhibitory effects.

Three-dimensional structures obtained from X-ray crystallography data of oxidized, reduced and partially reduced *Desulfovibrio gigas* AOR indicated that the major differences are in the structures of the Mo coordination complex and the Moco. The Mo^{VI} is reduced to Mo^{IV}, a substantial bond lengthening is observed for the apical sulfur ligand and the Mo deviates from the equatorial plane with 0.4 - 0.7 Å towards the apical ligand. In the reduced form the dithiolene sulfurs are also wider apart which results in a considerable puckering of the dithiolene molybdenum ring. Other structural differences are far from the molybdenum and presumably insignificant for the enzymatic reaction. There are no structural differences in the spatial arrangement of the amino acids in the substrate binding domains of the oxidized and reduced enzyme forms. Reduction of the Fe/S cofactors also resulted in no structural differences. Since the only major structural change in the active center involves the Mo^{IV}, it is most probably the factor that permits binding of the inhibitor to the E_{red} enzyme form. This is a reasonable assumption since 8-bromoxanthine has been shown to bind only to the E_{red} form.

When an inhibitor binds to the E_{ox} form of the enzyme it is clear that it competes with the xanthine for binding to the electron acceptor domain. With the inhibitor binding to the E_{red} form of the enzyme, it seems as if it is competing with the oxygen for a binding site. Oxygen is reduced at the FAD cofactor binding domain (electron donating) which is far from the electron acceptor domain. XO can potentially accommodate six reducing equivalents under anaerobic conditions and is thus able to complete three catalytic turnovers in the absence of oxygen. This means that xanthine is able to bind to the enzyme even if the Fe/S cofactors are in the reduced or partially reduced forms. It is possible that the same inhibitor can also compete with

xanthine for the electron acceptor domain of E_{red}. Alternatively it is possible that the binding of the inhibitor to E_{red} prevents the reducing equivalents from being transferred to oxygen.

Since polyphenols are structurally similar it is possible that they all might bind to the same binding site with varying affinities. Circumstantial evidence suggests that the polyphenols may bind to the electron acceptor domain. The XO enzyme is not very substrate specific and the basic structural requirements for substrates are the presence of aromatic heterocycles containing nitrogen or oxygen or a carbonyl group in the position α to the carbon that will be oxidized. The polyphenol EGCg exerts competitive inhibition with varying xanthine concentration. The secondary plots indicate linear competitive inhibition with the formation of a dead-end complex. All these results are indications that EGCg may bind to the electron acceptor domain of XO.

Models are proposed where the polyphenols and other structurally related inhibitors bind to the electron acceptor domain of either E_{ox} (Model A) or E_{red} (Model B) or to both forms of the enzyme (Model C) (Fig. 3.11). These models represent the initial reaction conditions where no products are present in the system. Under these conditions the product formation steps are far from equilibrium and essentially unidirectional. The reverse reaction where xanthine is produced from uric acid is also extremely slow and virtually non-existent. The water molecule that takes part in the reaction is ignored in the theoretical model. The reaction takes place in an aqueous medium where the concentration of water is not a rate-limiting factor. Two inhibitor constants K_I and K_i are used to define the affinity of the inhibitor for the oxidized or reduced forms of the enzyme respectively. The King-Altman procedure has been used

to derive the Alberty equation for each model. The inhibitory Alberty equation for each model will be derived mathematically.

King and Altman developed a schematic method for determining the rate laws for enzyme catalyzed reactions. For a scheme containing n enzyme forms *n* different steady-state equations are derived. The concentration of each enzyme form is defined as the sum of all the products of (*n-1*) rate constants and substrate concentrations (King, 1956).

Model A

Enzyme form	Paths forming enzyme form	Sum of *kappa* products
E_{ox}	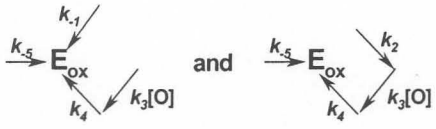	$k_{-1}k_3k_4k_{-5}[O]+k_2k_3k_4k_{-5}[O]$ $=(k_{-1}+k_2)k_3k_4k_{-5}[O]$
$E_{ox}X$	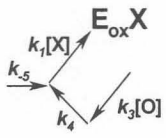	$k_1k_3k_4k_{-5}[X][O]$
E_{red}	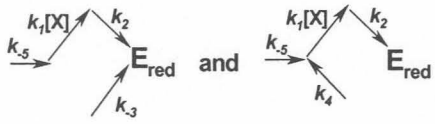	$k_1k_2k_{-3}k_{-5}[X]+k_1k_2k_4k_{-5}[X]$ $=(k_{-3}+k_4)k_1k_2k_{-5}[X]$
$E_{red}O$	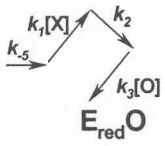	$k_1k_2k_3k_{-5}[X][O]$
$E_{ox}I$	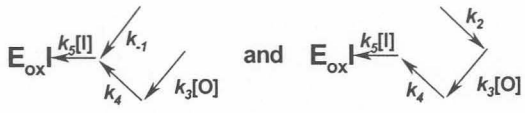	$k_{-1}k_3k_4k_5[O][I]+k_2k_3k_4k_5[O][I]$ $=(k_{-1}+k_2)k_3k_4k_5[O][I]$

$$E_{ox}X + E_{red}O = (k_2 + k_4)k_1k_3k_{-5}[X][O]$$

The enzyme reaction is monitored relative to uric aid formation. The reaction rate is defined by the equation: $v_0 = k_2[E_{ox}X]$

$$\frac{[E_{ox}X]}{[E_0]} = \frac{k_1k_3k_4k_{-5}[X][O]}{(k_{-3}+k_4)k_1k_2k_{-5}[X]+(k_{-1}+k_2)k_3k_4k_{-5}[O]+(k_{-1}+k_2)k_3k_4k_5[O][I]+(k_2+k_4)k_1k_3k_{-5}[X][O]}$$

$$v_0 = \frac{k_1k_2k_3k_4k_{-5}[E_0][X][O]}{(k_{-3}+k_4)k_1k_2k_{-5}[X]+(k_{-1}+k_2)(k_{-5}+k_5[I])k_3k_4[O]+(k_2+k_4)k_1k_3k_{-5}[X][O]}$$

$$v_0 = \frac{\left(\frac{k_2k_4}{k_2+k_4}\right)[E_0]k_1k_3k_{-5}[X][O]}{\left(\frac{k_{-3}+k_4}{k_2+k_4}\right)k_1k_2k_{-5}[X]+\left(\frac{k_{-1}+k_2}{k_2+k_4}\right)(k_{-5}+k_5[I])k_3k_4[O]+\left(\frac{k_2+k_4}{k_2+k_4}\right)k_1k_3k_{-5}[X][O]}$$

$$v_0 = \frac{\left(\frac{k_2k_4}{k_2+k_4}\right)[E_0][X][O]}{\frac{k_2}{k_3}\left(\frac{k_{-3}+k_4}{k_2+k_4}\right)[X]+\frac{k_4}{k_1}\left(\frac{k_{-1}+k_2}{k_2+k_4}\right)\left(\frac{k_{-5}+k_5[I]}{k_{-5}}\right)[O]+[X][O]}$$

For the ping-pong bi-bi system:

$$V_{max} = \left(\frac{k_2k_4}{k_2+k_4}\right)[E_0] \qquad K_m^X = \frac{k_4}{k_1}\left(\frac{k_{-1}+k_2}{k_2+k_4}\right)$$

$$K_m^{O_2} = \frac{k_2}{k_3}\left(\frac{k_{-3}+k_4}{k_2+k_4}\right) \qquad K_I = \frac{k_{-5}}{k_5}$$

$$v_0 = \frac{V_{max}[X][O]}{K_m^{O_2}[X]+K_m^X\left(1+\frac{[I]}{K_I}\right)[O]+[X][O]}$$

Under saturating O_2 conditions the Alberty equation can be reduced to a pseudo-single substrate Michaelis-Menten equation. This equation shows that inhibitors binding to the E_{ox} form (Model A) exhibits only competitive inhibition where V_{max} is unaffected and K_m is reduced.

$$v_0 = \frac{V_{max}[X]}{[X] + K_m^X\left(1 + \frac{[I]}{K_I}\right)}$$

Model B

Enzyme form	Paths forming enzyme form	Sum of *kappa* products
E_{ox}		$k_{-1}k_3k_4k_{-5}[O] + k_2k_3k_4k_{-5}[O] = (k_{-1} + k_2)k_3k_4k_{-5}[O]$
$E_{ox}X$	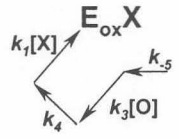	$k_1k_3k_4k_{-5}[X][O]$
E_{red}	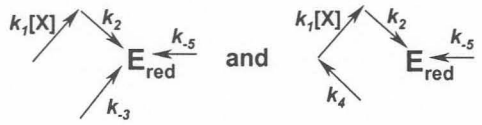	$k_1k_2k_{-3}k_{-5}[X] + k_1k_2k_4k_{-5}[X] = (k_{-3} + k_4)k_1k_2k_{-5}[X]$
$E_{red}O$	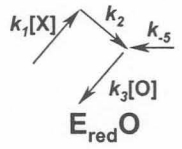	$k_1k_2k_3k_{-5}[X][O]$
$E_{red}I$	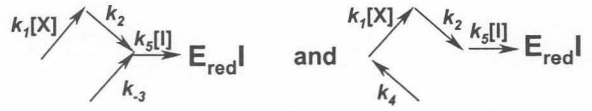	$k_1k_2k_{-3}k_5[X][I] + k_1k_2k_4k_5[X][I] = (k_{-3} + k_4)k_1k_2k_5[X][I]$

$$E_{ox}X + E_{red}O = (k_2 + k_4)k_1k_3k_{-5}[X][O]$$

$$\frac{[E_{ox}X]}{[E_0]} = \frac{k_1k_3k_4k_{-5}[X][O]}{(k_{-3}+k_4)k_1k_2k_{-5}[X]+(k_{-3}+k_4)k_1k_2k_5[X][I]+(k_{-1}+k_2)k_3k_4k_{-5}[O]+(k_2+k_4)k_1k_3k_{-5}[X][O]}$$

$$v_0 = \frac{k_1k_2k_3k_4k_{-5}[E_0][X][O]}{(k_{-3}+k_4)(k_{-5}+k_5[I])k_1k_2[X]+(k_{-1}+k_2)k_3k_4k_{-5}[O]+(k_2+k_4)k_1k_3k_{-5}[X][O]}$$

$$v_0 = \frac{\left(\frac{k_2k_4}{k_2+k_4}\right)[E_0]k_1k_3k_{-5}[X][O]}{\left(\frac{k_{-3}+k_4}{k_2+k_4}\right)(k_{-5}+k_5[I])k_1k_2[X]+\left(\frac{k_{-1}+k_2}{k_2+k_4}\right)k_3k_4k_{-5}[O]+\left(\frac{k_2+k_4}{k_2+k_4}\right)k_1k_3k_{-5}[X][O]}$$

$$v_0 = \frac{\left(\frac{k_2k_4}{k_2+k_4}\right)[E_0][X][O]}{\frac{k_2}{k_3}\left(\frac{k_{-3}+k_4}{k_2+k_4}\right)\left(\frac{k_{-5}+k_5[I]}{k_{-5}}\right)[X]+\frac{k_4}{k_1}\left(\frac{k_{-1}+k_2}{k_2+k_4}\right)[O]+[X][O]}$$

For model B the Alberty and pseudo-single substrate Michaelis-Menten equations indicate that inhibitor binding to the E_{red} form changes both K_m and V_{max} thus result in uncompetitive inhibition.

$$v_0 = \frac{\frac{V_{max}}{\left(1+\frac{[I]}{K_i}\right)}[X][O]}{K_m^O[X]+\frac{K_m^X}{\left(1+\frac{[I]}{K_i}\right)}[O]+[X][O]}$$

Alberty equation (Model B)

$$v_0 = \frac{\frac{V_{max}}{\left(1+\frac{[I]}{K_i}\right)}[X]}{[X]+\frac{K_m^X}{\left(1+\frac{[I]}{K_i}\right)}}$$

Michaelis-Menten equation (Model B)

Model C

Enzyme form	Paths forming enzyme form	Sum of *kappa* products
E_{ox}	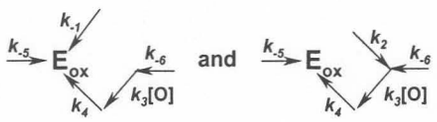	$k_{-1}k_3k_4k_{-5}k_{-6}[O]+k_2k_3k_4k_{-5}k_{-6}[O]$ $=(k_{-1}+k_2)k_3k_4k_{-5}k_{-6}[O]$
$E_{ox}X$	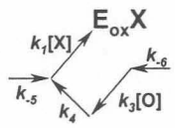	$k_1k_3k_4k_{-5}k_{-6}[X][O]$
E_{red}	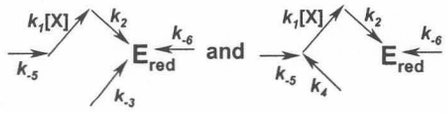	$k_1k_2k_{-3}k_{-5}k_{-6}[X]+k_1k_2k_4k_{-5}k_{-6}[X]$ $=(k_{-3}+k_4)k_1k_2k_{-5}k_{-6}[X]$
$E_{red}O$	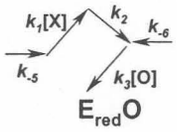	$k_1k_2k_3k_{-5}k_{-6}[X][O]$
$E_{red}I$	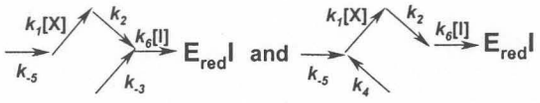	$k_1k_2k_{-3}k_{-5}k_6[X][I]+k_1k_2k_4k_{-5}k_6[X][I]$ $=(k_{-3}+k_4)k_1k_2k_{-5}k_6[X][I]$
$E_{ox}I$	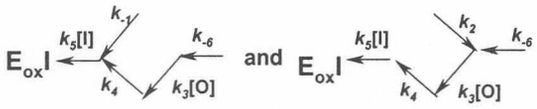	$k_{-1}k_3k_4k_5k_{-6}[O][I]+k_2k_3k_4k_5k_{-6}[O][I]$ $=(k_{-1}+k_2)k_3k_4k_5k_{-6}[O][I]$

$$\frac{[E_{ox}X]}{[E_0]}=\frac{k_1k_3k_4k_{-5}k_{-6}[X][O]}{(k_{-3}+k_4)(k_{-6}+k_6[I])k_1k_2k_{-5}[X]+(k_{-1}+k_2)(k_{-5}+k_5[I])k_3k_4k_{-6}[O]+(k_2+k_4)k_1k_3k_{-5}k_{-6}[X][O]}$$

$$v_0=\frac{k_1k_2k_3k_4k_{-5}k_{-6}[E_0][X][O]}{(k_{-3}+k_4)(k_{-6}+k_6[I])k_1k_2k_{-5}[X]+(k_{-1}+k_2)(k_{-5}+k_5[I])k_3k_4k_{-6}[O]+(k_2+k_4)k_1k_3k_{-5}k_{-6}[X][O]}$$

$$v_0=\frac{\left(\frac{k_2k_4}{k_2+k_4}\right)[E_0][X][O]}{\frac{k_2}{k_3}\left(\frac{k_{-3}+k_4}{k_2+k_4}\right)\left(\frac{k_{-6}+k_6[I]}{k_{-6}}\right)[X]+\frac{k_4}{k_1}\left(\frac{k_{-1}+k_2}{k_2+k_4}\right)\left(\frac{k_{-5}+k_5[I]}{k_{-5}}\right)[O]+[X][O]}$$

The Alberty and pseudo-single substrate Michaelis-Menten equation of Model C represent the non-competitive and mixed inhibition types. Two different inhibition constants are used for the defining the affinity of the inhibitor for E_{ox} and E_{red}.

$$v_0 = \frac{V_{max}[X][O]}{K_m^O[X]\left(1+\frac{[I]}{K_I}\right)+K_m^X[O]\left(1+\frac{[I]}{K_i}\right)+[X][O]}$$

Alberty equation (Model C)

$$v_0 = \frac{\frac{V_{max}}{\left(1+\frac{[I]}{K_I}\right)}[X]}{[X]+\frac{K_m^X\left(1+\frac{[I]}{K_i}\right)}{\left(1+\frac{[I]}{K_I}\right)}}$$

Michaelis-Menten equation (Model C)

The ratio K_i/K_I will be used to assess structure-affinity relationships of mixed type inhibitors. For $K_i/K_I < 1$ the inhibitor has a higher affinity for the E_{red} form than for the E_{ox} form of the enzyme. For $K_i/K_I = 1$ the inhibitor is a non-competitive inhibitor with equal affinity for both enzyme forms. For $K_i/K_I > 1$ the inhibitor has a higher affinity for the E_{ox} than E_{red} enzyme form.

3.3 Factors influencing apparent Ki values

The region in polyphenols that mimic the structures of other XO substrates will be named the primary binding region in polyphenols (Fig. 3.12). This region is defined as the A-ring together with the heterocyclic oxygen atom in the C-ring. Groups capable of forming hydrogen or coordination bonds are required in this region of the molecule. The orientation in itself does not determine whether the inhibitor binds to the E_{ox} or E_{red} enzyme forms preferentially. It does seem that at least one hydrogen bond forming group should be present on the positions C5-C7 on the A ring. Substi-

tution with methoxy or glycosyl groups in these positions reduces the affinity of the inhibitor for the enzyme. The affinity is increased when the heterocyclic oxygen atom is replaced with a nitrogen atom as found with purines.

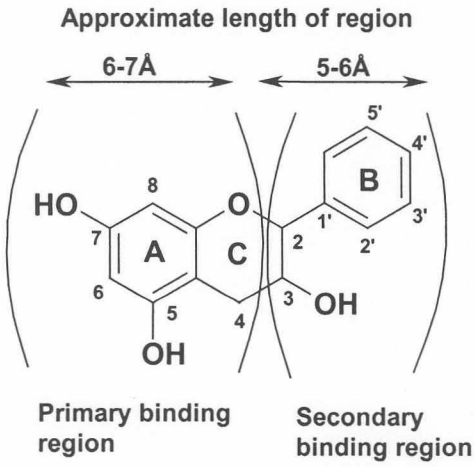

Figure 3.12 Polyphenols may have two regions that are important in defining their inhibitory effects on XO. The two regions are designated the primary and secondary binding regions.

The secondary binding region is defined as the rest of the polyphenol molecule. The function of this region is to enhance the inhibitor affinity and to modulate the ratio by which the inhibitor binds to the E_{ox} and E_{red} enzyme forms.

When comparing the inhibition constants (K_i) of synthetic pyrazolo-pyrimidine derivatives (Fig. 3.13A-C) (Springer, 1976), it was found that large aromatic groups as secondary binding regions increase the affinity of the enzyme for both forms of the enzyme. A similar pattern was observed for EC and ECG as well as for EGC and EGCg. (Fig. 3.13E-H). The extra aromatic gallate group increased the interaction of the secondary binding region with the enzyme resulting in increased affinities. The electron acceptor domains of AOR and XO are conserved with differences at only two residues.

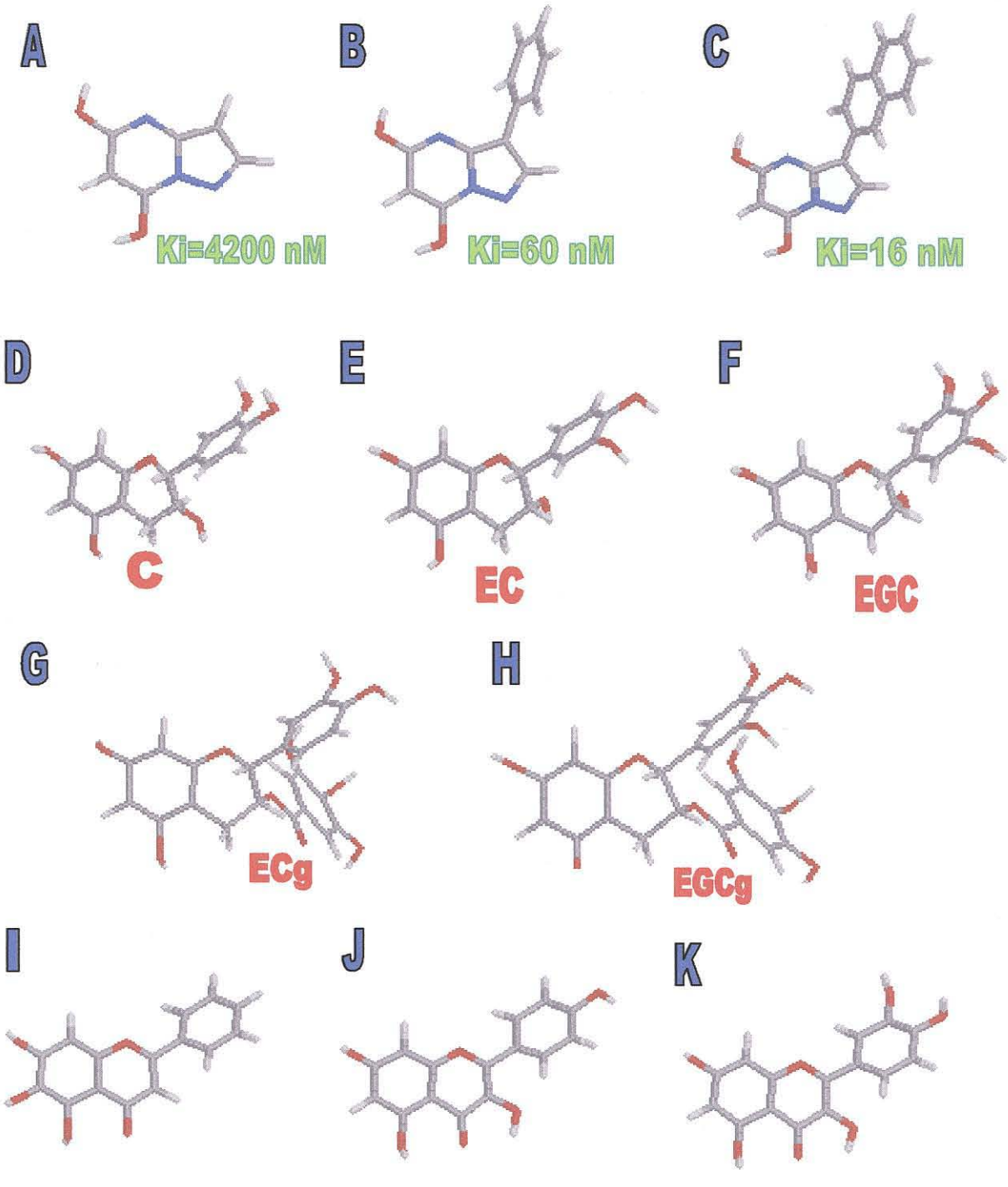

Figure 3.13 Structural similarities between synthetic pyrazolo-pyrimidines XO inhibitors and tea polyphenols. A structural pattern is observed between synthetic pyrazolo-pyrimidines (A-C) and tea polyphenols (E-H) that may explain the increase in affinity of inhibitor for the XO enzyme. Bulky secondary binding regions increase the affinity of the inhibitors for the enzyme. The pyrazolo-purine

inhibitors increase in potency from A to C. Likewise the gallated catechins, ECg (G) and EGCg (H), are also more potent inhibitors than the ungallated catechins, C (D), EC (E) and EGC (F). The three dimensional structures of bacalein (I), kaempferol (J) and quercetin (K) are also depicted. These inhibitors display the different structural properties that modulate the selective affinities of the inhibitors for the E_{ox} and E_{red} enzyme forms as discussed.

When studying the substrate binding or electron acceptor domain of AOR, (which is theoretically very similar to that of XO) it can be seen that it is funnel-shaped, about 15 Å deep and lined with hydrophobic moieties (Fig. 3.14). This explains why inhibitors with voluminous hydrophobic secondary binding regions have higher affinities (lower K_i). The primary binding region binds to the normal substrate binding residues near the Mo center at the base of the funnel. The secondary binding region of the inhibitor can then interact with the hydrophobic residues in the wider part of the substrate binding domain of XO. Larger secondary binding regions may fit more snugly in this cavity, allowing a larger surface for hydrophobic interaction and result in a higher affinity of the inhibitor for the enzyme. A schematic presentation is shown in Fig. 3.15.

The oxo-group on the C4 of bacalein, kaempferol and quercetin (Fig. 3.13I-K) also seems to bind to both forms of the enzyme since the affinity is significantly increased when this group is present. Bacalein is the uncompetitive inhibitor with the lowest K_I (2.48 μM) (Chang, 1993). The 1/Vmax vs [I] secondary plot of quercetin and kaempferol is parabolic non-linear. From this plot the K_I value is obtained indicating the affinity for the E_{ox} enzyme form. Parabolic non-linear secondary plots are observed when more than one inhibitor molecule binds per enzyme molecule. It is possible that polyphenols with an oxo group on C4 may bind to an additional site on the XO

enzyme. The secondary plot used for determining K_i is linear. This indicates that as with the other polyphenols a dead-end complex is formed with the E_{red} enzyme form.

3.4 Structural requirements for modulating K_i/K_I ratios

The K_i/K_I ratio is an indication of the affinity of the inhibitor for the E_{red} form relative to the E_{ox} form. For competitive inhibitors $K_i/K_I = \infty$ and for uncompetitive inhibitors $K_i/K_I = 0$. For true non-competitive inhibitors $K_i/K_I = 1$. Two regions seem to be important in altering the K_i/K_I ratios or XO inhibitors. The properties and orientations of the substituents on the C3 of the C-ring play an important role. A hydroxyl must be present and orientated in the plane of the C-ring or behind the plane in the (-)-configuration (epicatechin derivatives) (Fig. 3.13E-H) to allow the inhibitor to bind to the E_{ox} enzyme forms. A lack of a hydroxyl or a hydroxyl oriented towards the front of the C-ring plane leading to (+)-configuration (catechin) (Fig. 3.13D) only allows binding to the E_{red} enzyme form. When the hydroxyl in the (-)-configuration is substituted with a gallate, the K_i/K_I ratios increase significantly indicating that the inhibitor binds preferentially to the E_{ox} enzyme form. When EC is gallated to give ECg the K_i/K_I ratio jumps from 9.8 to 15.55 and when EGC with a ratio of 1.73 was changed to EGCg it was found to bind to the E_{ox} enzyme form only. Similarly, uric acid and 8-bromoxanthine (Fig. 3.10C and 3.10D) also have strong electronegative groups in the same region as the C3 hydroxyl group of the polyphenols. Both these two molecules only bind to the E_{red} enzyme form (uncompetitive inhibition). Binding studies of 8-bromoxanthine with XO showed that it binds only to the E_{red} enzyme form. The Mo is in the Mo^{IV} state and the bromine atom is 4 Å away from the molybdenum (Hille, 1984). The bromine atom is too far away from the Mo to form a direct bond and the nature of the interaction or the influence of bromine on the Mo center is

not understood. Xanthine and alloxanthine (oxypurinol) (Fig. 3.9A and 3.9B) lack hydroxyl groups in this region and bind to both forms of the enzyme.

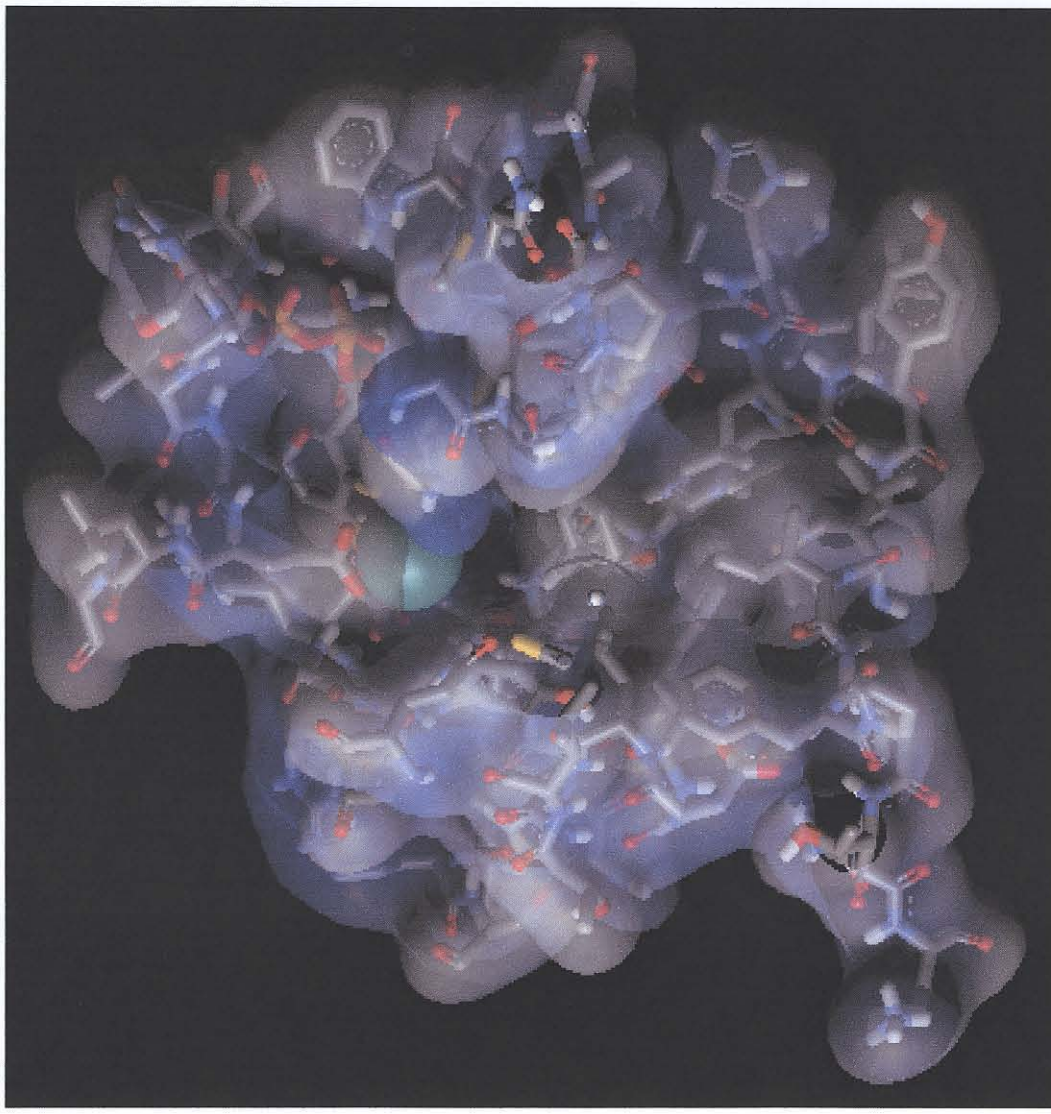

Figure 3.14 The substrate binding cavity of aldehyde oxido-reductase. The figure shows a cross-sectional view of the substrate binding domain with the mouth of the enzyme facing to the right. The substrate binding site is wide near the surface of the protein and gets narrower deeper into the enzyme core. Inhibitors with bulky secondary binding regions would presumably fit more tightly into the funnel shaped cavity.

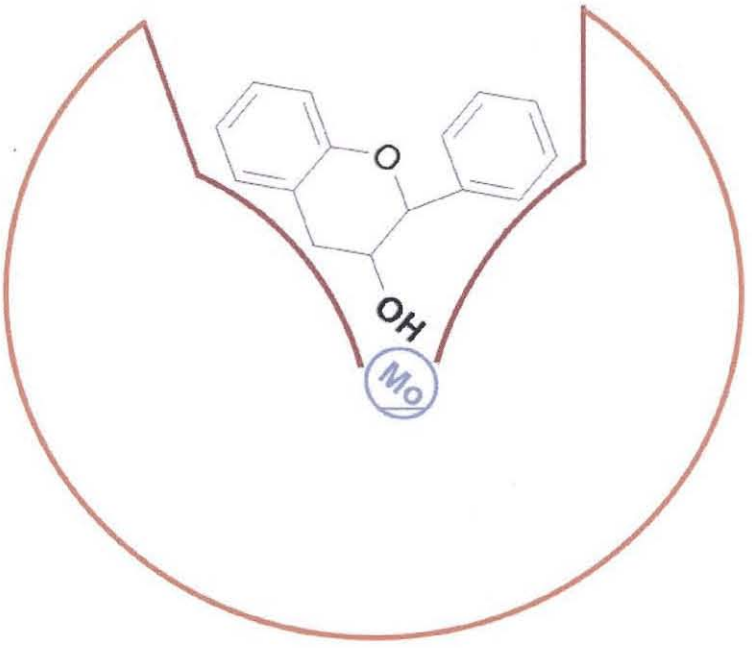

Figure 3.15 A schematic presentation of one way how the polyphenol may fit into the funnel-shaped active center of XO. The primary binding region of the inhibitor binds to the normal substrate recognition amino acids on one side. The secondary binding region interacts with the funnel wall and increases the affinity. The C3' OH is in close proximity of the Mo, resulting in an interaction that differentiates into competitive or uncompetitive inhibition.

The amount of hydroxylation on the B-ring also influences the selectivity of binding. The mono-hydroxylated kaempferol binds more selectively to the E_{ox} form (K_i/K_I = 4.85) than the di-hydroxylated quercetin (K_i/K_I = 2.65). Similarly the di-hydroxylated EC binds more selectively to the E_{ox} form (K_i/K_I = 9.8) than the tri-hydroxylated EGC (K_i/K_I = 1.73). Bacalein (Fig. 3.12I) with no hydroxyl groups on the B-ring does not bind to E_{ox} (uncompetitive) and tri-hydroxylated EGCg only binds to the E_{ox} form (competitive). Bacalein has no hydroxyl group on the C3 (consistent with uncompetitive inhibition) and EGCg has a gallated group on the C3 (resulting in preferential

binding to E_{ox}). This is a possible indication that the properties of the C3 are more important in determining the selectivity of binding than the hydroxylation pattern of the B-ring.

4 Conclusion

The tea polyphenols are good inhibitors of XO. The most potent inhibitor is EGCg and it compares well with allopurinol. Quercetin and kaempferol are two other polyphenols also showing inhibition of XO with similar potency as EGCg. Polyphenols and anthocyanidin extracts from other plants showed inhibition of XO (Costantino, 1992). This confirms our results of XO inhibition by the polyphenols. What is surprising is that compounds that are structurally similar can result in vastly different types of inhibition. The hypothetical model that is proposed is by no means the only possible explanation for the results obtained. The mathematical model and theory is sound and are commonly employed to elucidate multi-substrate mechanisms. It also agrees with experimental data obtained for the inhibition of XO with allopurinol and 8-bromoxanthine. Although it is understood that 8-bromoxanthine binds preferentially to the E_{red} enzyme form, it is not understood what interaction takes place between the bromine and the Mo. Similarly the interaction between the C8 OH of uric acid and the Mo center is unknown. Further studies of the interactions of the catechins with the XO enzyme may shed some light on the issue. It would be interesting to see whether catechin also binds in close proximity to the molybdenum center. This would prove conclusively whether catechin has a similar inhibitory mechanism as 8-bromoxanthine. This would place the hypothesis on firmer scientific grounds. The dimensions of the active centers of XO and AOR will most likely be very similar. Three-dimensional simulations of protein-ligand interactions with molecular modeling software

could also generate information of the interaction between XO and the catechins. One question that remains is whether polyphenols and coumarins can serve as substrates for XO or are they just molecules that have the ability to modulate the activity of the enzyme. Literature searches provided no published scientific evidence that polyphenols or coumarins are hydroxylated by XO.

A parallel can be drawn between XO and another liver enzyme, the cytochrome P450. The family of P450 mono-oxygenase enzymes catalyze hydroxylation reactions and also show low substrate specificity. Polyphenols have been shown to be able to modulate the activities of some of the P450 iso-enzymes by acting as inhibitors or allosteric activators (positive heterotropic cooperativity). In doing this, the polyphenols modulated the ability of the P450 enzymes to convert pro-carcinogens to carcinogenic or innocuous compounds. Inhibition of XO *in vivo* would lead to a reduced oxidative stress and this could explain some of the beneficial effects of tea on cancer and atherosclerosis that have been widely documented (Aucamp, 1997). If the *in vitro* results shown here could be repeated *in vivo*, tea polyphenols may become a novel treatment for gout.